THE NONLINEAR REGIME OF WAVEPACKETS IN PLANE POISEUILLE FLOW

HOMERO GHIOTI DA SILVA, ghioti@pontal.ufu.br
Faculdade de Ciências Integradas do Pontal - Universidade Federal de Uberlândia - FACIP/UFU Avenida José João Dib, 2545, cep. 38302-000, Iutiutaba-MG, Brazil

JOÃO BATISTA APARECIDO, jbaparecido@dem.feis.unesp.br
Faculdade de Engenharia de Ilha Solteira - Universidade Estadual Paulista- FEIS/UNESP Avenida Brasil, 56, centro, cep. 15385-000, Ilha Solteira-SP, Brazil

MARCELLO AUGUSTO FARACO DE MEDEIROS, marcello@sc.usp.br
Escola de Engenharia de São Carlos - Universidade de São Paulo - EESC/USP Av. trabalhador Sãocarlense, 400, cep. 13.560-970, São Carlos-SP, Brazil

Abstract. *Numerical and theoretical results of the natural transition in a plane Poiseuille flow were obtained in this work. Here the natural transition scenario was described by waves modulated in streamwise and spanwise directions. The natural transition is often studied in boundary layers, but the analysis in a parallel flow allows the use of the Reynolds number as a control parameter. Direct numerical simulation of the incompressible three-dimensional Navier-Stokes equations in a vorticity-velocity formulation was performed using numerical schemes with high order of accuracy. As the flow was parallel, a temporal analysis was considered. Two different situations were adopted. First, the scenario generated by interactions between wavepackets was investigated. Further, the isolated wavepacket was studied. The results indicated the scenario from interactions between wavepackets being the most likely scenario, where the oblique transition (described in literature) plays a role in natural transition and can lead to turbulent.*

Keywords: *Wavepacket, Numerical Simulation, High Order of Accuracy, Temporal Numerical Simulation, Plane Poiseuille Flow*

1. INTRODUCTION

Transition laminar-turbulent of fluids is a phenomenon of intense interest. In fact, prediction of laminar or turbulent flow is extremely important for applications in the aeronautical industry. It is necessary because the friction coefficient of the turbulent flow is much greater than that of the laminar flow. Consequently, the delay of transition from a laminar to turbulent flow may be important for reducing the viscous drag of aircraft in flight. This fact can reduce spending fuel and the size of aircraft. Furthermore, it increases the number of transported passengers number and the gain of airlines, (Joslin, 1998; Green, 2002; Boiko et al., 2002).

The flow transition occurs because the flow may be unstable for small perturbations. In fact, these perturbations generate systems of waves that develop along of the flow increasing in amplitude. In practical situations, the flow transition is called natural transition. There, the perturbations generate three-dimensional TS waves with modulation on spanwise and streamwise directions of the flow (three-dimensional wavepackets). In laboratory, wavepackets can be originated by a source point in the surface of the geometry and have been indicated by literature as a good technique for mimic the practical situation (Lele, 1992).

Due the high complexity for interpreting the natural transition, studies of simplified situations are performed. In fact, an important part of the study of flow transition involves the nonlinear interaction at two or three waves propagating in a boundary layer flow or plane Poiseuille flow. These simplified situations lead to three classical routes for the transition, the $K-$type and $H-$type transition and the oblique transition (Boiko et al., 2002). However, such simplified scenarios are much less complex than the natural transition, where many waves are present. These waves are modulated in streamwise and spanwise directions and result premature nonlinear activities (Gaster, 1978). Spikes and turbulent spots are often present in natural transition but the classical theory cannot anticipate these phenomena. Therefore, many questions remain regarding the relevance of these studies to natural transition. For instance, it is unknown whether such classical routes actually occur in natural transition, whether they occur simultaneously or interact, whether there is a dominant mechanism under some circumstances, etc.

The main proposal of this paper was to study the natural transition of the plane Poiseuille flow. The study has numerical and theoretical nature. So, a computational program of high order of accuracy was developed (Silva, 2008a). This code was submitted for some verification tests using the method of Manufactured Solutions (MMS) (Silva, 2008a; Silva et al., 2009). Also, numerical simulations and comparisons with results from the literature were performed and can be found in Silva (2008a).

One manner to study the natural transition is assuming only the spanwise modulation. This is done introducing perturbations able to generate three-dimensional wavetrains in the flow. They result scenarios more complex than those presented in the literature but less complex than that generated by wavepackets. The wavetrains allow only studying the three-dimensionality of the flow. This characteristic of the flow can give important informations on the natural transition. Medeiros (2004) studied the nonlinear regime of spanwise modulated wavetrains in a boundary layer flow. In that study, Medeiros (2004) observed a modified oblique transition, which was a seed for the growth of the $K-$type transition. Silva (2008a); Silva and Medeiros (2008) studied the nonlinear regime of spanwise modulated wavetrains in plane Poiseuille Flow. Silva (2008a); Silva and Medeiros (2008) observed two nonlinear regimes that also could be attributed to classical scenarios. However, in plane Poiseuille flow, the nonlinear regime occurred separately for different regions of the instability diagram. In cases near the first branch of the diagram, the oblique transition was dominant for the nonlinear regime. On the other hand, far the first branch, the $K-$type transition takes over. The results showed that both scenarios could be attributed to classical scenarios described in literature. However, the nonlinear regime of wavetrains in plane Poiseuille flow could not be similar to those results reached in Medeiros (2004). In fact, as explained above, the nonlinear regime of the plane Poiseuille flow was dominated by classical scenarios of transition, but not in the same parameters. It is contrary to the case boundary layer flow, where a modified oblique transition was a seed for dominance of $K-$type transition. Other differences between them were reported in Silva and Medeiros (2008).

The studies of wavetrains motivated the analysis of more complex situations, where wavepackets in the flow. Medeiros (2006) studied the nonlinear regime of isolated wavepackets in boundary layer. The results suggested that the three classical scenarios of transition, indicated above, can occur simultaneously. In fact, the wavepackets analysis was an extension that performed for three-dimensional wavetrain. Despite that such behavior was much more complex than the wavetrains, Medeiros (2006) observed the presence of each classical scenario of transition in different stages of the nonlinear regime. Firstly, a modified oblique transition was observed. This first nonlinear stage was a seed to the nonlinear second stage, which was dominated by $K-$type transition. It was similar to the results reaching in Medeiros (2004). However, it was possible to identify a third nonlinear stage, more advanced, where the $H-$type transition dominated the process.

Similar studies, but in plane Poiseuille flow, were performed in this paper. Here, two different scenarios for transition were identified. One scenario was resulted from interactions between wavepackets. Another scenario was resulted from the evolution of isolated wavepackets. The results suggested that the first scenario may be the most relevant scenario for natural transition because it is often present in practical situations.

The current paper is presented as follows. In section 2 governing equations and boundary conditions for the physical problem in question, are shown. In this same section, a fast explanation for the adopted numerical scheme is presented. Choice of the initial conditions and parameters are explained in section 3. Section 4 presents results of these studies. Final remarks are presented in the section 5.

2. GOVERNING EQUATIONS, BOUNDARY CONDITIONS AND NUMERICAL METHOD

The governing equations describe an incompressible and three-dimensional flow between two plates. In this paper, the governing equations were written in a vorticity-velocity formulation, where the Navier/Stokes equations are used for transport of vorticity $\vec{\omega}$ in the interior of the domain, as follow:

$$\frac{\partial \vec{\omega}}{\partial t} = (\vec{\omega} \cdot \nabla)\vec{u} - \vec{u} \cdot \nabla \vec{\omega} + \frac{1}{Re}\nabla^2 \vec{\omega}, \tag{1}$$

where the components of $\vec{\omega}$ are:

$$\omega_x = \frac{\partial v}{\partial z} - \frac{\partial w}{\partial y}, \quad \omega_y = \frac{\partial w}{\partial x} - \frac{\partial u}{\partial z}, \quad \omega_z = \frac{\partial u}{\partial y} - \frac{\partial v}{\partial x}. \tag{2}$$

From the definition of vorticity, Eq. (2), and using the fact that both velocity and vorticity vector fields are solenoidal, namely,

$$\nabla \cdot \vec{u} = 0, \quad \nabla \cdot \vec{\omega} = 0, \tag{3}$$

one obtains the Poisson equation for the velocity field as follow

$$\nabla^2 \vec{u} = -\nabla \times \vec{\omega}. \tag{4}$$

A periodic boundary condition was adopted in both streamwise and spanwise directions (x and $z-$directions). For the wall normal direction ($y-$direction), non-slip and impermeability ($u = v = w = 0$ at the walls) conditions were imposed. The flow geometry is presented in Fig. 1.

As the flow was parallel, a temporal analysis was considered. The equations cited above were rewritten to the Fourier space and solved using numerical schemes with mixed high order of accuracy. In fact, for streamwise and spanwise directions of the flow, the discretization of the equations was performed using pseudo-spectral methods. For the normal

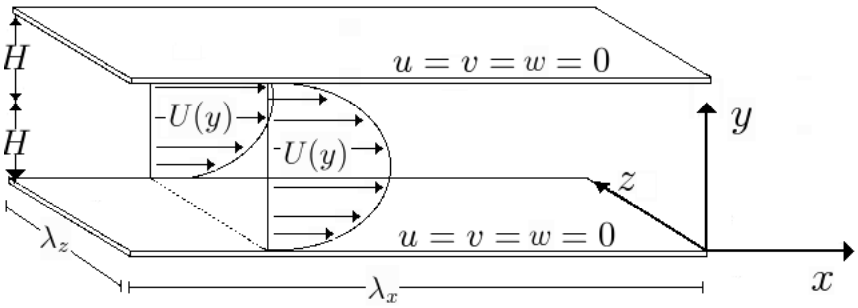

Figure 1. Schematic diagram of the physical system.

direction of the flow, mixed high-order compact finite difference schemes were used. The temporal integration was performed with a Runge-Kutta method of 4^{th} order of accuracy except to mean flow distortion calculations, where Runge-Kutta of the 4^{th} order of accuracy and Crank Nicolson methods were necessary to assure numerical stability. Full details of the chosen numerical scheme can be found in (Silva, 2008a) and (Silva and Medeiros, 2008).

3. INITIAL CONDITION AND CHOOSE OF THE PARAMETERS

The initial condition was generated using the current numerical code. Initially, a disturbance was introduced into computational domain through a technique of type blowing or suction, as used in experimental procedures Laurien and Kleiser (1989); Marxen (1998). In this technique, the wall normal velocity v has the following expression

$$v(x, y_0, z, t) = A^{(m,n)}(1 - cos(2\pi\frac{t - t_1}{t_2 - t_1}))\Re(e^{i(\alpha^n x+\beta^m z+\phi^{(n,m)})}), \tag{5}$$

where $A^{(m,n)}$, α^n, β^m and $\phi^{(n,m)}$ indicate, respectively, amplitude, streamwise and spanwise wavenumbers and phase for the disturbance (n, m). The $\Re$ symbol indicates the real part of the complex number $e^{i(\alpha^n x+\beta^m z+\phi^{(n,m)})}$. Here, y_0 assumes the values 0 and $2H$.

In order to avoid possible nonlinear mechanisms during the generation of the initial condition, only the linear terms of the governing equations were simulated. The disturbance (5) converged to Tollmien-Schlichting waves (TS waves), which are solutions of the Navier-Stokes equations in a linearized version (Boiko et al., 2002). The linearized Navier-Stokes equations are fundamental for the Linear Stability Theory (LST), and result the Orr-Sommerfeld equation, which was solved numerically, for example, by Mendonça (2003). Some comparisons between the propagation of TS waves, using the current initial condition, and the LST were performed and found in Silva (2008a).

The figure shows the linear instability diagram for TS waves.

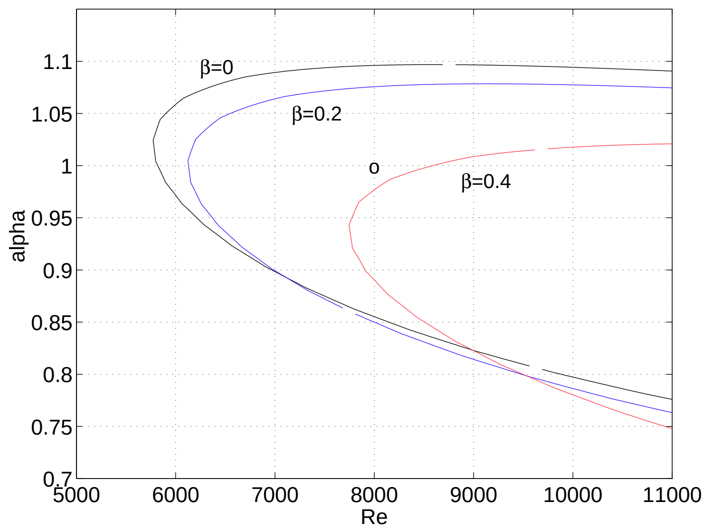

Figure 2. Linear Stability Diagram of the two and three-dimensional TS waves.

It was plotted as streamwise wavenumber versus Reynolds number values ($\alpha \times Re$). Each curve indicated (neutral curve) into the diagram corresponds to one set of TS waves. For example, the curve $\beta = 0$ represents the two-dimensional

TS waves that satisfy null linear growth rate. So, the two-dimensional TS waves located inside of the region limited by curve $\beta = 0$ increase in amplitude. On the other hand, the two-dimensional TS out of this region and not located at the curve, the reverse situation occurs. This explanation also can be validated for other cases of β values.

In the present work, the chosen initial condition covered the discrete range of streamwise and spanwise wavenumbers set to $0 \leq \alpha \leq 1.72 \times -1.72 \leq \beta \leq 1.72$. Each TS wave had initial amplitude set to $A = 2 \times 10^{-5}$. The chosen Reynolds number was set to $Re = 8000$. Details about the initial condition and the motivation for choosing it can be found in Silva (2008a) and Silva (2008b).

Figure 3 displays the initial condition in both physical (left) and Fourier (right) spaces.

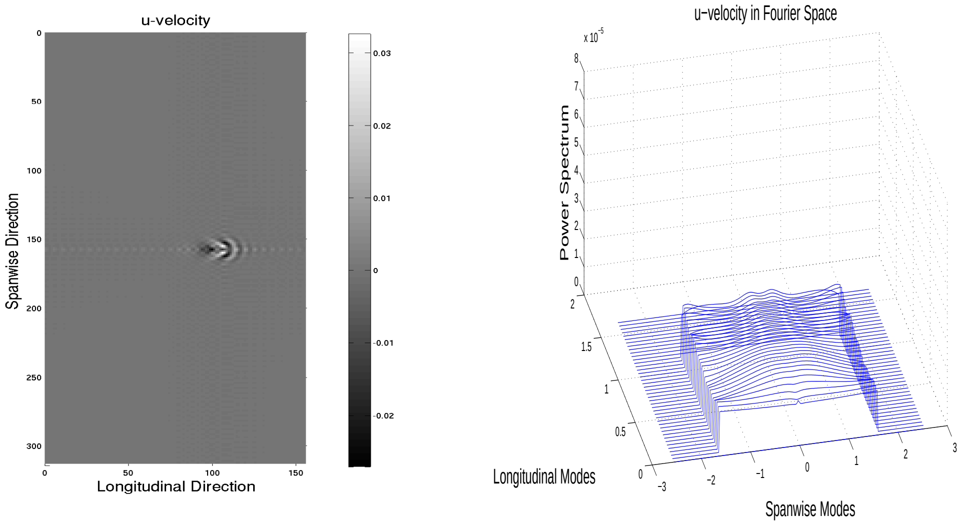

Figure 3. Initial condition for present simulations.

Note in fig. 3 a modulation in both streamwise and spanwise directions of the wavepacket in physical space. This fact occurred because of the use of a big number of Fourier modes applied in the flow. The initial condition was spectrum flat, although the figure 3 (right) not indicates it. This occurred because the maximal amplitude of each Fourier mode is located at different points in normal direction of the flow. Here, the results were recorded only from fixed value $0.11H$ in normal direction of the flow. More details for this explanation can be found in Silva (2008a).

A mesh refinement test was performed in the present work (not shown in this paper). It can be found in Silva (2008a). The optimal mesh and parameters for both Fourier and physical spaces were presented in the Tab. 4.

Table 1. Parameters for the present study[a].

Parameters for the Fourier Space		Parameters for the physical Space	
N_x	85	n_x	128
α_0	0.04	λ_x	$(0\,,\,2\pi/\alpha) = (0\,,\,157.07)$
N	201	N	201
N_z	85	n_z	128
β_0	0.04	λ_z	$(-2\pi/\beta\,,\,2\pi/\beta) = (-157.07\,,\,157.07)$

The parameters α_0 and β_0 are the smallest streamwise and spanwise wavenumbers able to be simulated using this resolution. n_x, N, n_z denote, respectively, the number of points used at streamwise, normal and spanwise directions for physical space discretization. N_x and N_z are numbers of Fourier modes at streamwise and spanwise directions. Note that the x and $z-$directions resolution for the Fourier space was smaller than the physical space only to avoid alias error (Press et al., 1992).

4. NUMERICAL RESULTS

Figure 4 displays the temporal evolution of the $u-$velocity for the three-dimensional wavepacket. The results were obtained from the wall normal position $y = 0.11H$. They were recorded in the adimentional times set to $356, 763, 1144$ and 1450. Initially the wavepacket was strongly concentrated on the centerline of the domain or $z = 0$. During the linear regime of the flow, the wavepacket satisfied a dispersion relation (Silva, 2008a) spending a larger portion of the flow field. However, after $t = 1114$, it was possible to identify interactions between adjacent wavepackets. Such scenario is different

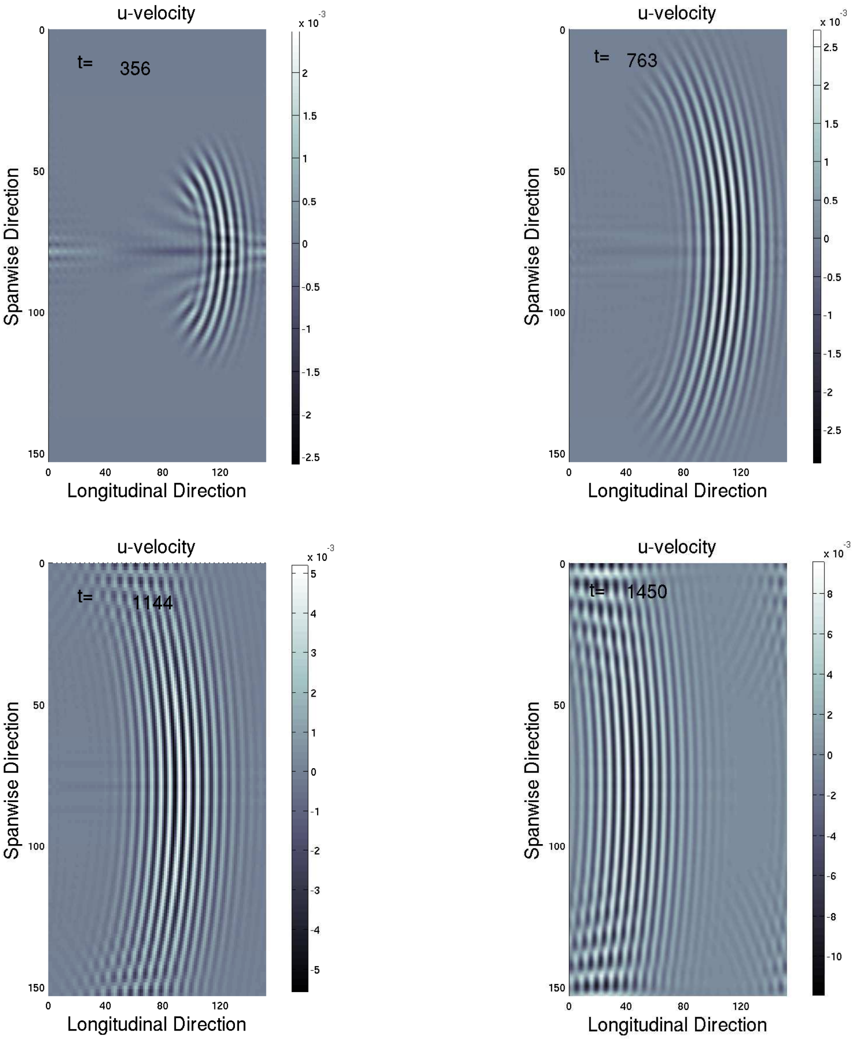

Figure 4. Time evolution for $u-$velocity of the wavepacket in a short physical space in spanwise direction.

of a scenario where the wavepacket evolves separately. Nevertheless, it is very important because it describes a typical situation in natural transition. In attempt to understand the nonlinear regime of the flow, an analysis of the Fourier space was performed.

The analysis in the physical space is interesting, but the analysis in the Fourier space can give more information from the nonlinear regime of the flow. Figure 5 displays the temporal evolution of the Fourier modes in a spectral domain. The results were recorded in adimentional times similar to the Fig. 4. Along of temporal evolution it was indentified Fourier modes increasing in amplitude according to Linear Instability Theory (Boiko et al., 2002). So, around of $t = 1144$, some spanwise-periodic Fourier modes satisfying α near and at the zero were presents. These Fourier modes had peaks at the modes $\alpha = 0$ and $\beta = -1$ and 1, respectively. In the nonlinear regime, such peaks had the largest amplification rate and confirmed such scenario as dominant for this case. This scenario resembled the oblique transition.

A study of the nonlinear regime of isolated wavepacket was also done. For this objective, a numerical simulation was performed using the same parameters indicated in table 1 except to the β_0 value, which was set to 0.02. Therefore, the length of the domain in spanwise direction was longer than that shown in fig. 4. Figure 6 displays the temporal evolution of the $u-$velocity for the three-dimensional wavepacket in physical space. The results were also obtained from the wall normal position $y = 0.11H$. Indeed, they are recorded in adimentional times similar to fig. 4. The start of the temporal evolution was similar to that shown in fig. 4. In fact, the wavepacket was strongly concentrated on the centerline of the domain or $z = 0$ and satisfied a dispersion relation (Silva, 2008a). Around of time $t = 1450$ it was possible to identify some flow distortions near centerline of the domain. These distortions may not be described by the Linear Stability Theory and, therefore, the weakly nonlinear mechanisms may be present in the flow. Figure 7 displays the temporal evolution of the Fourier modes in a spectral domain. The results confirmed a dispersion relation from linear regime of the flow. In fact, it was possible to indentify the Fourier modes increasing in amplitude according to Linear Instability Theory (Boiko

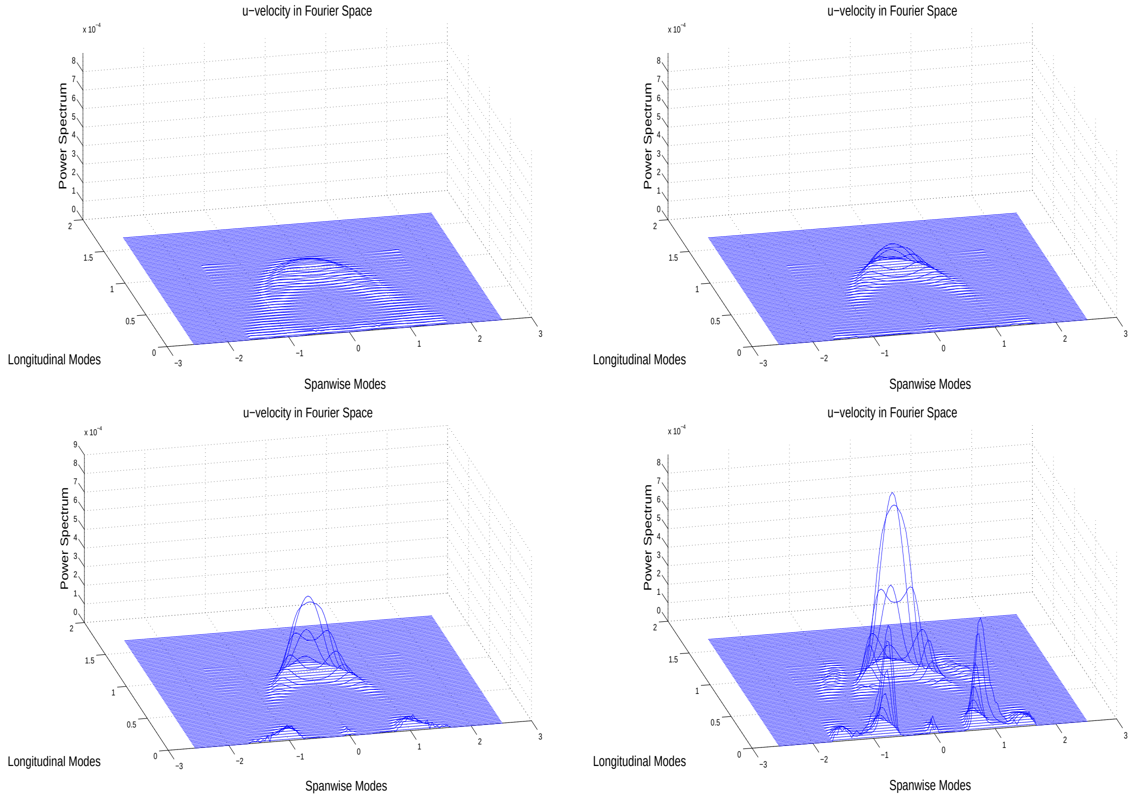

Figure 5. Time evolution of the Fourier modes for the $u-$velocity. *Top left:* $(0, N_z\beta)$ modes. *Top right:* $(\alpha, N_z\beta)$ modes. *Lower:* $(2\alpha, N_z\beta)$ modes.

et al., 2002). However, around of $t = 1144$, other spectral modes had appeared in the spectral domain. First, spectral modes satisfying near and at null streamwise wavenumber were present. After, other spectral ranges around of $\beta = -1.2$ and 1.2 and several α values were also amplified. This behavior cannot be predicted by Linear Instability Theory. They may be increasing because of nonlinear interactions in the flow. Furthermore, they may be the cause of the distortions near centerline of the flow, as pointed by results in the physical space, fig. 6.

Such results not pointed the dominance at isolated classical nonlinear scenario, $K-$ or $H-$ type instabilities or oblique transition. In fact, it was not possible to identify some dominance by oblique modes, as occur in oblique transition. However, although the results showed some spectral ranges of harmonics and subharmonics modes, it can be hard to identify the dominance of $H-$ or $K-$ type instabilities. Nevertheless, other explanation for this scenario is the presence of the three scenarios simultaneously. This possibility cannot be discarded and other studies of this case should be performed.

Another flow instability, still not mentioned in this paper, is the dominance of the flow by detuned modes (Herbert, 1988). Such scenario involves the resonant combination of symmetrical oblique modes at the near subharmonic values amplifying another pair of symmetrical oblique waves at the 'mirror streamwise wavenumber'. The fig. 7, in adimentional time $t = 1450$, presents generated Fourier modes by nonlinear regime satisfying properly such concept. In fact, in particular to positive Fourier modes, the three dimensional waves around $\alpha = 0.7$ and $\beta = 1.2$ may be generated by symmetrical waves around $\alpha = 0.3$ and $\alpha = 1.1$. Similar behavior for the negative Fourier modes.

5. FINAL REMARKS

The paper reports an investigation of the natural transition in a plane Poiseuille flow. It was performed numerical simulations of the linear and weakly nonlinear regime of wavepacket generated by perturbations imitating blowing and suction in the flow. The wavepacket was composed of a sufficient number of TS waves to cover a discrete range of the Fourier modes linearly unstables. Indeed, it satisfied a Reynolds number at $Re = 8000$ and was of very small amplitude.

Two different situations were adopted. First, a transition scenario caused by interactions between wavepackets was studied. This scenario is important because it is concerning to the practical situation, where different source points of perturbations generated different wavepackets that, in some moment of the flow evolution, can be interacting between them. Further, choosing a sufficient spanwise length to the Fourier domain, the temporal evolution of an isolated wavepacket was also investigated.

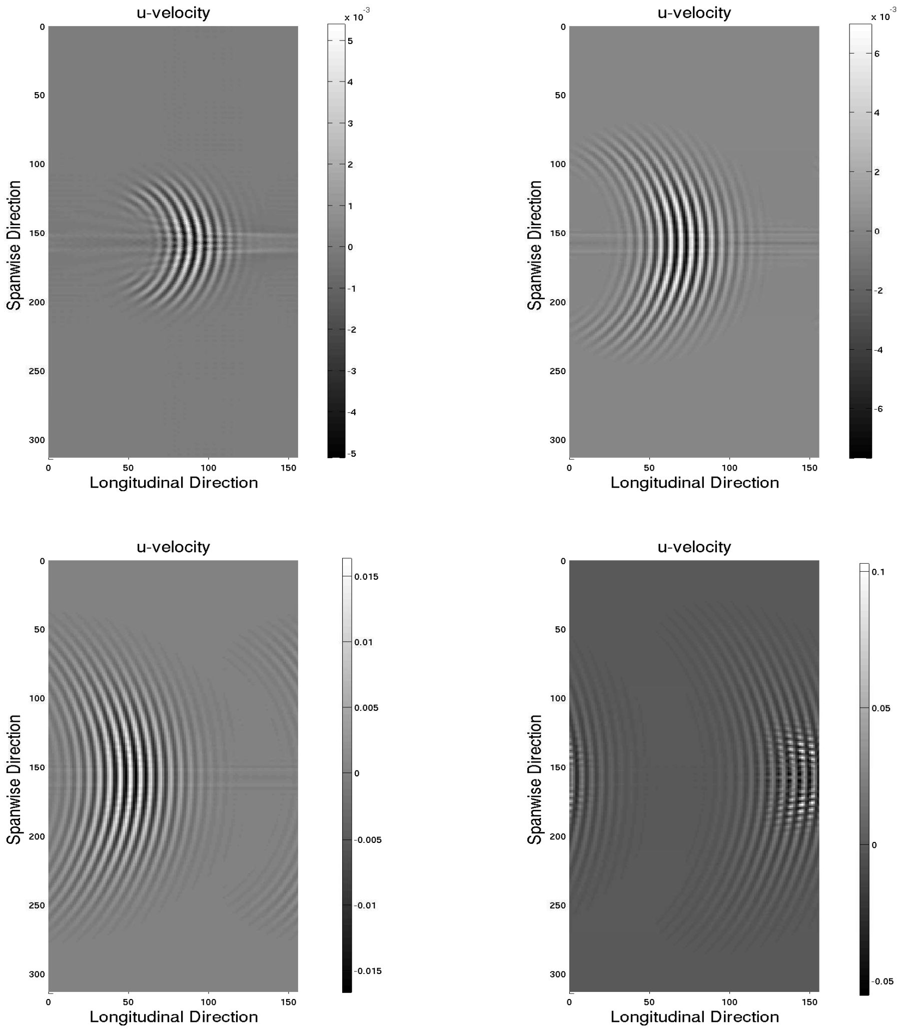

Figure 6. Time evolution of the $u-$velocity of a wavepacket in the plane Poiseuille flow at $y = 0.11H$. Results obtained from the physical space.

The results suggested that the nonlinear regime from interactions between wavepackets was dominated by a modified oblique transition scenario. In fact, the nonlinear regime of the flow was dominated by some waves satisfying streamwise wavenumber near and at null. They presented two peaks located at two stationary spanwise-periodic waves, satisfying $\alpha = 0$ and $\beta = -1$ and 1. These modes can be resulted from nonlinear interactions between oblique waves, as occur in oblique transition. However, the oblique transition is generated from two oblique waves only, which is different of the present case where there were a large number of waves of different streamwise and spanwise wavenumber. There, the present result can be assumed as a modified oblique transition.

The scenario of the isolated wavepacket in the plane Poiseuille flow had different behavior to the nonlinear regime, when compared with the scenario of interactions between wavepackets. On the other hand, it was more complex than those classical scenarios described in literature. In fact, although the results in physical space have suggested some distortions around of centerline of the flow, it may not be associated with longitudinal streaks, as occur to oblique transition. Indeed, it was not identified some dominant oblique wave in the Fourier space. Flow distortions around of centerline was also identified in the wavetrains in plane Posieuille flow (Silva and Medeiros, 2008). However, those flow distortions were strongly concentrated in the centerline of the flow, different of the present result. In that work, the cause to those flow distortions was the dominance of $K-$type transition. In the present results, the flow distortions were less concentrated around the centerline of the flow. Although the results indicated the presence of fundamental modes and subharmonics modes in the nonlinear regime, it is difficult to identify the dominance of the $K-$ or $H-$ type transition. On the other hand, the results indicated strongly characteristic of detuned modes, but this conjecture need verifications in future works.

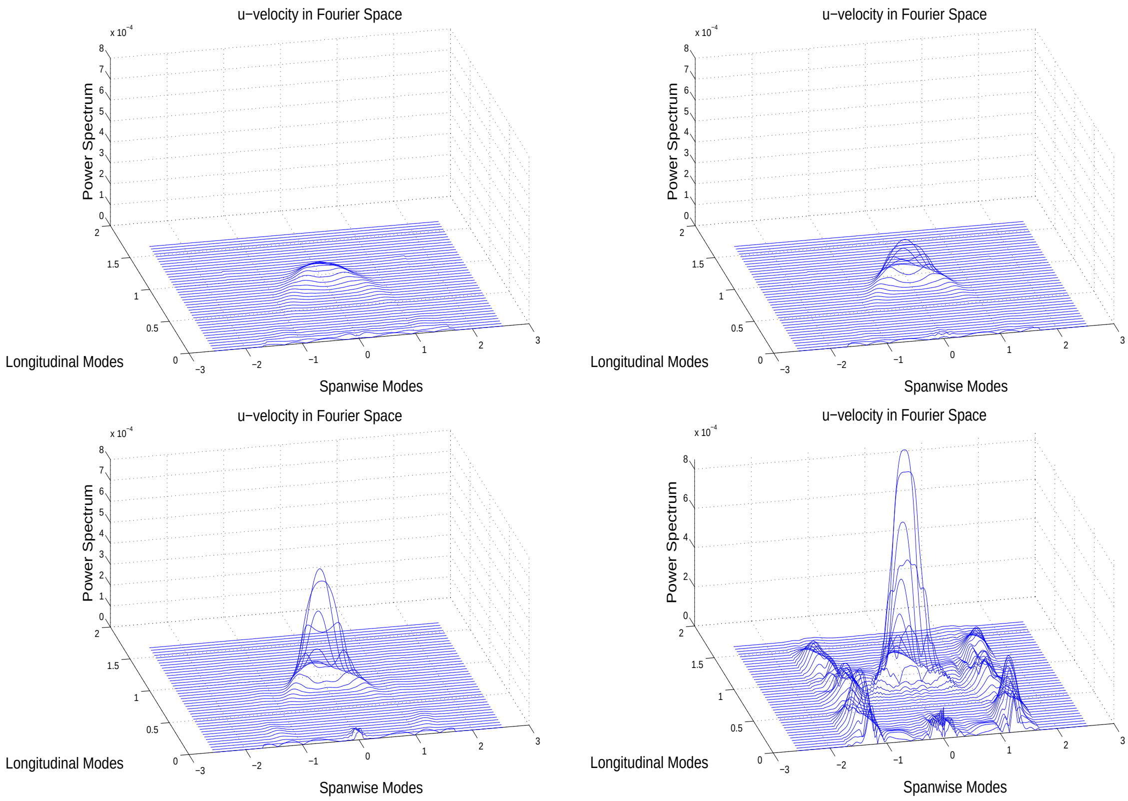

Figure 7. Time evolution of the Fourier modes for the $u-$velocity. *Top left:* $(0, N_z\beta)$ modes. *Top right:* $(\alpha, N_z\beta)$ modes. *Lower:* $(2\alpha, N_z\beta)$ modes.

6. ACKNOWLEDGEMENTS

The financial support of the AFSOR, CNPq and FAPESP are gratefully aknowledged.

7. REFERENCES

A. Boiko, G. Grek, A. V. Dovgal, and V. Koslov. *The Origin of Turbulence in Near-Wall Flows*. Springer-Verlag, Berlim, Germany, 2002.

M. Gaster. The physical process causing breakdown to turbulence. In *Naval Hydrodinamics Symposium*, Washington, 1978.

J. Green. Greener by design. *The Aeronautical Journal*, (1056):57–114, 2002.

T. Herbert. Secondary instability of boundary-layers. *Ann. Rev. Fluid Mechanics*, 20:487–526, 1988.

R. Joslin. Aircraft laminar flow control. *Annu. Rev. Fluid. Mech*, 30:1–29, 1998.

E. Laurien and L. Kleiser. Numerical simulation of boundary-layer transition control. *J. Fluid Mech.*, 199:403–440, 1989.

S. Lele. Compact finite difference schemes with spectral-like resolution. *Journal of Computational Physics*, 103:16–42, 1992.

O. Marxen. *Temporal Direct Numerical Simulation of a Flat Plate Boundary Layer, Diplomarbeit*. PhD thesis, University of Arizona, Arizona-USA, 1998.

M. Medeiros. The nonlinear evolution of a wavetrain emanating from a point source in a boundary layer. *J. Fluid Mech.*, 508:287–317, 2004.

M. Medeiros. *Os Primeiros Estágios Não-Lineares da Transição Natural em Camada Limite (livre-docência)*. Universidade de São Paulo-Escola de Engenharia de São Carlos-Departamento de Engenharia de Materiais, Aeronáutica e Automobilística, São Carlos, S.P., Brasil, 2006.

M. T. Mendonça. *Estabilidade de Escoamentos de Laminares: Teoria Linear, capítulo 5*. ABCM-EPTT, Uberlândia-MG, 2003.

W. H. Press, S. A. Teukolsky, W. T. Vetterling, and V. P. Flannery. *Numerical Recipies in Fortran 77*. Cambridge University Press, Cambridge, 1992.

H. Silva. *Regime Não Linear de Trens de Ondas Modulados na Direção Transversal em um Escoamento de Poiseuille Plano*. PhD thesis, Escola de Engenharia de São Carlos, Universidade de São Paulo, São Carlos, S.P., Brazil, 2008a.

H. Silva and M. A. Medeiros. Nonlinear regime of a spanwise modulated wavetrain in a plane poiseuille flow. In *Escola de Primavera de Transição e Turbulência-EPTT*, São Carlos, Brazil, 2008.

H. G. Silva, L. Souza, and M. Medeiros. On the verification of a mixed high-order accurate DNS code by the method of manufactured solutions - ACCEPTED FOR PUBLICATION. *Int. J. Num. Meth. Fluids*, pages –, 2009.

8. Responsibility notice